References

[1] Theodore S. Rappaport, **“Wireless Communications Principle and Practice”**, Prentice Hall, 2nd Edition, 2002.

[2] Ron Schmitt,**”Electromagnetics Explained”**, Elsevier Science (USA), 2002.

[3] Online Education, **“Smart Antenna Systems”**, International Engineering Consortium, 2003. http://www.iec.org/online/tutorials/smart_ant/topic01 .html

[4] Lal Chand Godara, “**Smart Antennas**”, CRC Press, 2004.

[5] Hussein Zarei, **“RF Variable Phase shifters for Multiple Smart Antenna Transceivers”**, Ph.D. Dissertation, Department of Electrical Engineering, University of Washington, 2004.

[6] Anderson, V.C. and Rudnick P., **“Rejection of a Coherent Arrival at an Array”**, J. Acoust. Soc. Am., pp. 406–410, 1969.

[7] Anderson and V.C., **“DICANNE, a Realizable Adaptive Process”**, J. Acoust. Soc. Am., pp. 398–405, 1969.

[8] S. Jeng, G. Xu, H. P. Lin, and W. J. Vogel, **“Experimental Studies of Spatial Signature Variation at 900 MHz for Smart Antenna Systems”**, IEEE Transactions on Antennas and Propagation, 1998.

[9] A. Paulraj, R. Roy, and T. Kailath, **“A Subspace Rotation Approach to Signal Parameter Estimation”**, Proceedings of the IEEE, 74(7):1044–1045, July 1986.

[10] Garret T. Okamoto, **“Smart Antenna Systems and Wireless LANs”**, Kluwer Academic Publishers, 2002.

[11] Kok Keng Ng, **“Smart Antenna Application in DS-CDMA Mobile Communication System”**, M.SC thesis, Naval Postgraduate School, September 2002

[12] William G. Newhall, **“Radio Channel Measurements and Modeling for Smart Antenna Array Systems Using a Software Radio Receiver”**, Ph.D. Dissertation, Bradley Department of Electrical and Computer Engineering, Virginia Tech, Blacksburg, Virginia, April 2003.

[13] Ahmed Al Zooghby, **“Smart Antenna Engineering”**, Artech House Mobile Communication Series, ISBN-10: 1-58053-515-1, 2002.

[14] Garret T. Okamoto, **“Smart Antenna Systems and Wireless LANs”**, Kluwer, Academic Publishers, ISBN: 0-306-47323-2, 2002.

[15] Sammy Kayali, George Ponchak, and Roland Shaw, **“Ga As MMIC Reliability Assurance Guideline for Space Applications”**, Jet Propulsion Laboratory California Institute of Technology Pasadena, California, JPL Publication 96-25, December 15, 1996.

[16] Nadim Maluf, and Kirt Williams,**“An Introduction to Microelectromechanical Systems Engineering”**, 2nd edition, Artech house Microelectromechanical Systems series, ISBN 1-58053-590-9, 2004.

[17] Héctor J. De Los Santos,**”RF MEMS Circuit Design for Wireless Communications”**, Artech house Microelectromechanical Systems series, ISBN 1-58053-329-9, 2002.

[18] Justin L. Serraiocco, Peter J. Hansen*, Troy R. Taylor*, James S. Speck*, and Robert A. York, **“Compact Ferroelectric Reflection Phase Shifters at X-Band”**, Electrical and Computer Engineering Dept, University of California, Santa Barbara, Ca, 93106, USA. (*Materials Dept)

[19] Röbert A. York, Amit S. Nagra, and Padmini Periaswamy**,” Synthesis and Characterization of $(Ba_XSr_{1-X})Ti_{1+Y}O_{3+Z}$ Thin Films and Integration Into Microwave Varactors and Phase Shifters “**,Department of Electrical and Computer Engineering ,University of California-Santa Barbara, Santa Barbara, CA 93106 .

[20] Yu Liu[a], Baki Acikel[a], Amit S. Nagra[a], Troy R. Taylor[b], Peter J. Hansen[b], James S. Speck[b], and Robert A. York[a], **” Distributed Phase Shifters Using $(Ba,Sr)TiO_3$ Thin Films on Sapphire and Glass Substrates”**, [a]Electrical and Compute Engineering Department, [b]Materials Department, University of California, Santa Barbara, California, 93106, 2001.

[21] B. Acikel, T. R. Taylor, P.J. Hansen, J. S. Speck, and R. A. York, **“A New High performance Phase Shifter using $Ba_XSr_{1-X}TiO_3$ Thin Films”**, *ÏEEE Microwave and Wireless Component Letters*”, vol. MTT-12, no.7, pp.237-239, July 2002.

[22] D. Kim, Y. Choi, M. G. Allen, J. S. Kenney, and D. Kiesling, **"Ä Wide Bandwidth Monolithic BST Reflection Type Phase Shifter Using a Coplanar waveguide Lange Coupler"**, 2002 *IEEE MTT-S International Microwave Symposium Digest*., vol. 3, pp.1471-1474, June 2002.

[23] Liam Devlin, **"The Design of Integrated Switches and Phase Shifters",** Plextek Communications Technology Consultants, 1999. http://www.plextek.compapers/swdes2.pdf

[24] Rf RFIC & Microwave Theory Design, **"Phase Shifter Design Tutorial"**, 2004.http://www.odyseus.nildram.co.uk/RFMicrowave_Circuits_Files/Phase_%20Shifter.pdf

[25] Amit S. Nagra and Robert A. York, **"Distributed Analog Phase Shifters with Low Insertion Loss"**, IEEE Transactions on microwave theory and techniques, VOL. 47, NO. 9, Sept. 1999.

[26] W. M. Zhang, R. P. Hsia, C. Liang, G. Song, C. W. Domier, and N. C. Luhmann, Jr., **"Novel low-loss delay Line for Broadband Phased Antenna Array Applications",** IEEE Microwave Guided Wave Lett., vol. 6, pp. 395–397, Nov. 1996.

[27] A. S. Nagra and R. A. York, **"Monolithic GaAs Phase Shifter with Low Insertion Loss and Continuous 0_–360_ Phase Shift at 20 GHz",** IEEE Microwave Guided Wave Lett., vol. 9, pp. 31–33, Jan. 1999.

[28] M. J. W. Rodwell, M. Kamegawa, R. Yu, M. Case, E. Carman, and K. S. Giboney, **"GaAs Nonlinear Transmission Lines for Picosecond Pulse Generation and Millimeter-wave Sampling",** IEEE Trans. Microwave Theory Tech., vol. 39, pp. 1194–1204, July 1991.

[29] U. Bhattacharya, S. T. Allen, and M. J. W. Rodwell, **"DC-725 GHz Sampling Circuits and Subpicosecond Nonlinear Transmission Lines Using Elevated Coplanar Waveguide,"** IEEE Microwave Guided Wave Lett., vol.5, pp. 50–52, Jan. 1995.

[30] Andrea Borgioli, Yu Liu, Amit S. Nagra, and Robert A. York, **"Low-Loss Distributed MEMS Phase Shifter"**, IEEE MICROWAVE AND GUIDED WAVE LETTERS, VOL. 10, NO. 1, JANUARY 2000

[31] Frank Ellinger, Rolf Vogt, and Werner Bächtold, **“Compact Reflective-Type Phase-Shifter MMIC for C-Band Using a Lumped-Element Coupler”**, IEEE TRANSACTIONS ON MICROWAVE THEORY AND TECHNIQUES VOL. 49, NO. 5, MAY 2001

[32] Frank Ellinger, , Rolf Vogt, and Werner Bächtold, **“Ültracompact Reflective-Type Phase Shifter MMIC at C-Band with 360° Phase-Control Range for Smart Antenna Combining”**, IEEE JOURNAL OF SOLID-STATE CIRCUITS, VOL. 37, NO. 4, APRIL 2002.

[33] Garvin Cung and Paul Lee, **“RF/Microwave Circuit for Phase Shifting in Phased Antenna Arrays**”, ECE 345, SENIOR DESIGN PROJECT, Spring 2003.

[34] Frank Ellinger, Rolf Vogt and Werner Bächtold, “**A high Yield Ultra Small Passive Vector Modulator Based Phase Shifter for Smart Antenna Combining at C-Band”**, Swiss Federal Institute of Technology (ETH) Zurich, 2000.

[35] Frank Ellinger, **“An antenna Diversity MMIC Vector Modulator for HIPERLAN with low power Consumption and Calibration Capability”**, IEEE transactions on microwave theory and techniques, Vol.49, No.5, May 2001.

[36] Frank Ellinger, Urs Lott and Werner Bächtold, “**A Calibratable 4.8-5.8 GHz MMIC Vector Modulator with Low Power consumption for Smart Antenna Receivers”**, Swiss Federal Institute of Technology (ETH) Zurich, 2000.

[36] Onsemi, “MMBF5460LT1.pdf”, http://www.onsemi.com/PowerSolutions /product.do?id=MMBF5460LT1

[37] Anadigics, ÄWS5522.pdf”, http://www.anadigics.com/products/addrefs/ Datasheet/AWS5522 Rev0.1.pdf

[38] Amplifonix, “TWP2233”, Spectrum Microwave, http://www.amplifonix.Com /pdf/switch / TWHP2233.pdf

[39] Amplifonix, “TWH5017”, Spectrum Microwave, http://www.amplifonix. Com/pdf/switch / TWH5017.pdf

Appendix A

Simulation Results

A.1 AC Analysis results

Table A.1 AC Analysis results for the Directional Coupler

	X--Trace 1::[$1] Frequency(Hz)	Y--Trace 1::[$1] Phase(deg)
1.	1	1.899076353
2.	1.258925412	1.508693791
3.	1.584893192	1.198500238
4.	1.995262315	0.952053752
5.	2.511886432	0.756268776
6.	3.16227766	0.600738408
7.	3.981071706	0.477189796
8.	5.011872336	0.379048391
9.	6.309573445	0.301090244
10.	7.943282347	0.239165022
11.	10	0.189975594
12.	12.58925412	0.15090275
13.	15.84893192	0.119865874
14.	19.95262315	0.095212215
15.	25.11886432	0.075628915
16.	31.6227766	0.06007311
17.	39.81071706	0.047716409
18.	50.11872336	0.037900775
19.	63.09573445	0.030103493
20.	79.43282347	0.02390933
21.	100	0.018988426
22.	125.8925412	0.015078725
23.	158.4893192	0.011972021
24.	199.5262315	0.00950287
25.	251.1886432	0.007539782
26.	316.227766	0.005978215
27.	398.1071706	0.004735009
28.	501.1872336	0.00374396
29.	630.9573445	0.00295229
30.	794.3282347	0.002317841
31.	1000	0.001806825
32.	1258.925412	0.001392029

	X--Trace 1::[$1] Frequency(Hz)	Y--Trace 1::[$1] Phase(deg)
33.	1584.893192	0.001051363
34.	1995.262315	0.000766687
35.	2511.886432	0.000522839
36.	3162.27766	0.000306835
37.	3981.071706	0.000107171
38.	5011.872336	-8.67866E-05
39.	6309.573445	-0.000285365
40.	7943.282347	-0.000499141
41.	10000	-0.000739498
42.	12589.25412	-0.001019235
43.	15848.93192	-0.001353251
44.	19952.62315	-0.001759332
45.	25118.86432	-0.002259104
46.	31622.7766	-0.002879182
47.	39810.71706	-0.003652586
48.	50118.72336	-0.004620505
49.	63095.73445	-0.005834481
50.	79432.82347	-0.007359166
51.	100000	-0.009275752
52.	125892.5412	-0.011686306
53.	158489.3192	-0.014719199
54.	199526.2315	-0.018535943
55.	251188.6432	-0.023339792
56.	316227.766	-0.029386571
57.	398107.1706	-0.036998291
58.	501187.2336	-0.046580303
59.	630957.3445	-0.058642883
60.	794328.2347	-0.073828404
61.	1000000	-0.092945545
62.	1258925.412	-0.11701235
63.	1584893.192	-0.14731044
64.	1995262.315	-0.185453251
65.	2511886.432	-0.233471928
66.	3162277.66	-0.293923446
67.	3981071.706	-0.370026682
68.	5011872.336	-0.465833634
69.	6309573.445	-0.586444829
70.	7943282.347	-0.738280169
71.	10000000	-0.92941929
72.	12589254.12	-1.170028778
73.	15848931.92	-1.472897499
74.	19952623.15	-1.854105524

	X--Trace 1::[$1] Frequency(Hz)	Y--Trace 1::[$1] Phase(deg)
75.	25118864.32	-2.333856311
76.	31622776.6	-2.937504573
77.	39810717.06	-3.696811086
78.	50118723.36	-4.651445024
79.	63095734.45	-5.850723548
80.	79432823.47	-7.355507232
81.	100000000	-9.240023906
82.	125892541.2	-11.59311997
83.	158489319.2	-14.51798201
84.	199526231.5	-18.12875538
85.	251188643.2	-22.54207897
86.	316227766	-27.86276002
87.	398107170.6	-34.1695898
88.	501187233.6	-41.53061568
89.	630957344.5	-50.16627708
90.	794328234.7	-61.53882079
91.	1000000000	72.71439854
92.	1258925412	-58.97507873
93.	1584893192	-75.20449723
94.	1995262315	-97.41786854
95.	2511886432	168.6507796
96.	3162277660	122.7661766
97.	3981071706	111.3937634
98.	5011872336	105.6248266
99.	6309573445	101.8901645
100.	7943282347	99.221348

A.2 Results of Phase Shifter Circuit (Capacitive Load)

Table A.2 Phase shift versus control voltage for the Capacitive Load circuit

	Control Voltage (V)	Phase Shift Angle (deg)
1.	0	-130.016
2.	0.1	-129.838
3.	0.2	-129.441
4.	0.3	-129.06
5.	0.4	-128.071
6.	0.5	-126.373
7.	0.6	-124.472
8.	0.7	-122.524
9.	0.8	-120.587

	Control Voltage (V)	Phase Shift Angle (deg)
10.	0.9	-118.675
11.	1	-116.804
12.	1.1	-114.968
13.	1.2	-113.198
14.	1.3	-111.473
15.	1.4	-109.798
16.	1.5	-108.181
17.	1.6	-106.614
18.	1.7	-105.083
19.	1.8	-103.638
20.	1.9	-102.23
21.	2	-100.852
22.	2.1	-99.556
23.	2.2	-98.296
24.	2.3	-97.079
25.	2.4	-95.907
26.	2.5	-94.777
27.	2.6	-93.676
28.	2.7	-92.633
29.	2.8	-91.625
30.	2.9	-90.652
31.	3	-89.713
32.	3.1	-88.807
33.	3.2	-87.934
34.	3.3	-87.091
35.	3.4	-86.278
36.	3.5	-85.493
37.	3.6	-84.735
38.	3.7	-83.984
39.	3.8	-83.282
40.	3.9	-82.602
41.	4	-81.944
42.	4.1	-81.306
43.	4.2	-80.689
44.	4.3	-80.092
45.	4.4	-79.513
46.	4.5	-78.952
47.	4.6	-78.409
48.	4.7	-77.882
49.	4.8	-77.371
50.	4.9	-76.876
51.	5	-76.395

	Control Voltage (V)	Phase Shift Angle (deg)
52.	5.1	-75.928
53.	5.2	-75.475
54.	5.3	-75.035
55.	5.4	-74.608
56.	5.5	-74.192
57.	5.6	-73.788
58.	5.7	-73.396
59.	5.8	-73.013
60.	5.9	-72.642
61.	6	-72.28
62.	6.4	-70.924
63.	6.6	-70.297
64.	7	-69.113
65.	7.4	-68.06
66.	7.6	-67.569
67.	8	-66.649
68.	8.5	-65.604
69.	9	-64.662
70.	9.5	-63.807
71.	10	-63.03
72.	10.5	-62.319
73.	11	-61.668
74.	11.5	-61.068
75.	12	-60.515
76.	12.5	-60.305
77.	13	-59.527
78.	13.5	-59.084
79.	14	-58.671
80.	15	-57.923
81.	16	-57.264
82.	17	-56.678
83.	18	-56.155
84.	20	-55.259
85.	22	-54.521
86.	24	-53.902
87.	26	-53.376
88.	30	-52.529
89.	32	-52.183
90.	35	-51.737
91.	40	-51.138

A.3 Results of Phase Shifter Circuit (Dual Capacitive Load)

Table A.3 Phase shift versus control voltage for the Dual Capacitive Load circuit

	Control Voltage (v)	Phase Shift Angle (deg)
1.	0	147.439
2.	0.1	146.529
3.	0.2	145.585
4.	0.3	144.653
5.	0.4	144.06
6.	0.5	143.786
7.	0.6	143.603
8.	0.7	143.443
9.	0.8	143.284
10.	0.9	143.116
11.	1	142.935
12.	1.1	142.737
13.	1.2	142.521
14.	1.3	142.288
15.	1.4	142.034
16.	1.5	141.762
17.	1.6	141.468
18.	1.7	141.159
19.	1.8	140.829
20.	1.9	140.48
21.	2	140.108
22.	2.1	139.727
23.	2.2	139.327
24.	2.3	138.91
25.	2.4	138.478
26.	2.5	138.031
27.	2.6	137.57
28.	2.7	137.096
29.	2.8	136.61
30.	2.9	136.102
31.	3	135.598
32.	3.1	135.084
33.	3.2	134.561
34.	3.3	134.031
35.	3.4	133.493
36.	3.5	132.95
37.	3.6	132.403
38.	3.7	131.851
39.	3.8	131.297

	Control Voltage (v)	Phase Shift Angle (deg)
40.	3.9	130.741
41.	4	130.185
42.	4.1	129.627
43.	4.2	129.071
44.	4.3	128.516
45.	4.4	127.963
46.	4.5	127.413
47.	4.6	126.866
48.	4.7	126.323
49.	4.8	125.784
50.	4.9	125.251
51.	5	124.723
52.	5.1	124.201
53.	5.2	123.685
54.	5.3	123.176
55.	5.4	122.674
56.	5.5	122.157
57.	5.6	121.672
58.	5.7	121.194
59.	5.8	120.723
60.	5.9	120.261
61.	6	119.806
62.	6.4	118.069
63.	6.6	117.251
64.	7	115.713
65.	7.4	114.304
66.	7.6	113.646
67.	8	112.419
68.	8.5	111.043
69.	9	109.81
70.	9.5	108.733
71.	10	107.774
72.	10.5	106.922
73.	11	106.166
74.	11.5	105.492
75.	12	104.892
76.	12.5	104.349
77.	13	103.873
78.	13.5	103.444
79.	14	103.059
80.	15	102.397
81.	16	101.855

	Control Voltage (v)	Phase Shift Angle (deg)
82.	17	101.409
83.	18	101.038
84.	20	100.464
85.	22	100.057
86.	24	99.759
87.	26	99.536
88.	30	99.24
89.	32	99.141
90.	35	99.032
91.	40	98.919

A.4 Simulation results using resonating loads of 15 nH:

Table A.4 Phase shift versus control voltage using 15 nH inductors

	Control Voltage (v)	Phase Shift Angle (deg)
1.	0	10.269
2.	0.5	09.193
3.	1.5	07.848
4.	2.0	07.103
5.	2.5	06.375
6.	3.0	05.699
7.	3.5	05.094
8.	4.5	04.117
9.	6.0	03.152
10.	11	02.034
11.	15	01.862

A.5 Simulation results using resonating loads of 10 nH:

Table A.5 Phase shift versus control voltage using 10 nH inductors

	Control Voltage (v)	Phase Shift Angle (deg)
1.	0	33.761
2.	0.1	33.168
3.	0.2	32.570
4.	0.3	31.984
5.	0.4	31.539
6.	0.5	31.221
7.	0.6	30.936

	Control Voltage (v)	Phase Shift Angle (deg)
8.	0.7	30.655
9.	0.8	30.370
10.	0.9	30.077
11.	1	29.776
12.	1.2	29.155
13.	1.4	28.507
14.	1.6	27.842
15.	1.8	27.168
16.	2	26.493
17.	2.2	25.824
18.	2.4	25.168
19.	2.6	24.528
20.	2.8	23.909
21.	3	23.315
22.	3.2	22.746
23.	3.4	22.204
24.	3.6	21.690
25.	3.8	21.204
26.	4	20.746
27.	4.5	19.718
28.	5	18.843
29.	5.5	18.104
30.	6	17.481
31.	6.5	16.956
32.	7	16.513
33.	7.5	16.139
34.	9	15.322
35.	10	14.900
36.	15	14.119
37.	16	14.047
38.	17	13.800

A.6 Simulation results using resonating loads of 6.8 nH:

Table A.6 Phase shift versus control voltage using 6.8 nH inductors

	Control Voltage (v)	Phase Shift Angle (deg)
1.	0	62.202
2.	0.1	61.271
3.	0.2	60.328
4.	0.3	59.400
5.	0.4	58.691

	Control Voltage (v)	Phase Shift Angle (deg)
6.	0.5	58.180
7.	0.6	57.720
8.	0.7	57.267
9.	0.8	56.807
10.	0.9	56.336
11.	1	55.851
12.	1.2	54.849
13.	1.4	53.802
14.	1.6	52.723
15.	1.8	51.624
16.	2	50.519
17.	2.2	49.419
18.	2.4	48.335
19.	2.6	47.274
20.	2.8	46.244
21.	3	45.250
22.	3.2	44.297
23.	3.4	43.387
24.	3.6	42.522
25.	3.8	41.703
26.	4	40.929
27.	4.5	39.188
28.	5	37.705
29.	5.5	36.450
30.	6	35.391
31.	6.5	34.499
32.	7	33.746
33.	7.5	33.109
34.	9	31.721
35.	10	31.098
36.	15	29.663
37.	16	29.539

A.7 Simulation results using resonating loads of 3.3 nH:

Table A.7 Phase shift versus control voltage using 3.3nH inductors

	Control Voltage (v)	Phase Shift Angle (deg)
1.	0	106.518
2.	0.1	105.339

	Control Voltage (v)	Phase Shift Angle (deg)
3.	0.2	104.133
4.	0.3	102.941
5.	0.4	102.079
6.	0.5	101.518
7.	0.6	101.038
8.	0.7	100.571
9.	0.8	100.097
10.	0.9	99.607
11.	1	99.095
12.	1.2	98.014
13.	1.4	97.281
14.	1.6	95.594
15.	1.8	94.277
16.	2	92.905
17.	2.2	91.493
18.	2.4	90.054
19.	2.6	88.602
20.	2.8	87.151
21.	3	85.712
22.	3.2	84.297
23.	3.4	82.913
24.	3.6	81.570
25.	3.8	80.272
26.	4	79.025
27.	4.5	76.143
28.	5	73.611
29.	5.5	71.417
30.	6	69.534
31.	6.5	67.925
32.	7	66.554
33.	7.5	65.386
34.	9	62.810
35.	10	61.645
36.	15	58.933
37.	16	58.698

Appendix B

Components Specification

B.1 MMBF5460LT1 Specifications

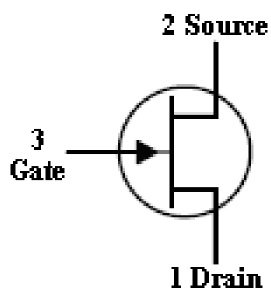

Figure B.1 Symbol and package for MMBF5460LT1

Table B.1 Maximum Ratings for MMBF5460LT1:

Rating	Symbol	Value	Unit
Drain-Gate Voltage	V_{DG}	40	V_{dc}
Reverse Gate-Source Voltage	V_{GSR}	40	V_{dc}
Forward Gate Current	I_{GF}	10	mA_{dc}

Table B.2 Thermal Characteristics for MMBF5460LT1:

Characteristic	Symbol	Max	Unit
Total Device Dissipation FR-5 board, (Note 1) T_A= 25°C	P_D	225 1.8	mW mW/°C
Thermal Resistance, Junction-to-Ambient	$R_{\theta JA}$	556	
Junction and storage Temperature	T_J, T_{stg}	-55 to +150	

B.2 AWS5522 Specifications

The AWS5522 is a single pole, double throw (SPDT) RF switch developed to meet the stringent requirements of GSM and CDMA systems. Manufactured in ANADIGICS's state-of-the-art pHEMT process, the device uses patent-pending circuit topologies to provide the low insertion loss, high port-to-port isolation and high linearity needed to enhance the performance of wireless handset radios. The AWS5522 is offered both as an MMIC die and in a 12-lead 3mm x 3mm package.

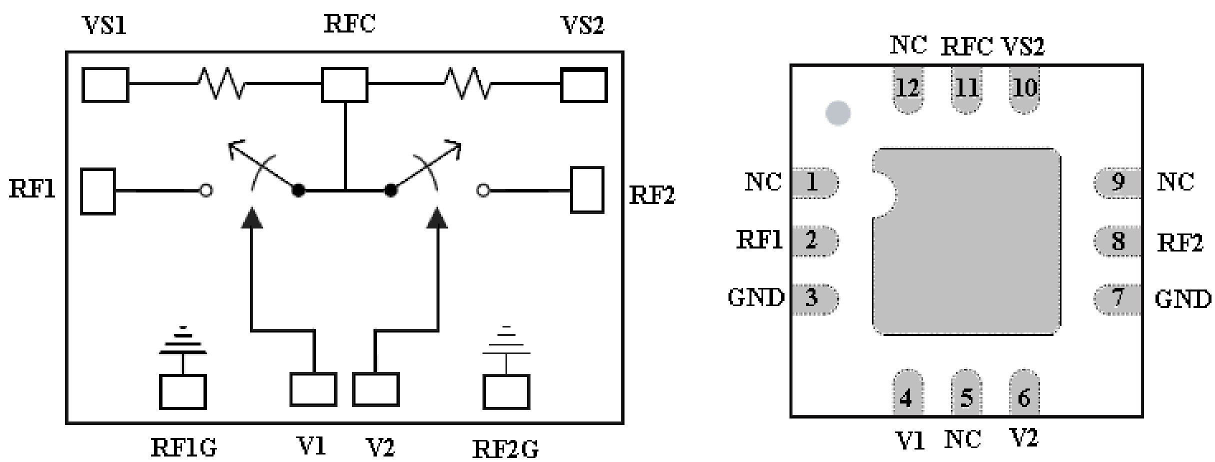

Figure B.2 Block Diagram of the AWS5522 chip and Packaged Device Pin Layout

Table B.3 Pin Description

Pin	Name	Description
2	Rf1	RF port, path1
4	V1	Control voltage, RF path 1
6	V2	Control voltage, RF path 2
8	Rf2	RF port, path 2
10	VS2	Common port bias Voltage (logic high)
11	RFC	RF common port
3,7	GND	Ground
1,5,9,12	NC	No connection

Table B.4 AWS5522 Specifications

Specifications	
Package	D1
Frequency (GHz)	2.5
Isolation (dB)	25-27
P1dB (dBm)	-
IP3 (dBm)	-
Control Voltage Operation	Positive to +2.5V
Insertion loss (dB)	0.8 dB
Type	SP4T

Table B.5 Switch Control Truth Table:

Control Voltages		**RF Path Selection**	
V_1	**V_2**	**RFC-RF1**	**RFC-RF2**
+2.5 to +3.5 V	0 to +0.2V	ON	OFF
0 to +0.2V	+2.5 to +3.5 V	OFF	ON

Table B.6 Absolute Minimum and Maximum Ratings:

Parameter	**Min**	**Max**	**Unit**	**Comments**
Common Port Bias Voltage (V_S)	-0.2	+8.0	V	At VS1 or VS2
Control Voltages (V_1,V_2)	-0.2	+8.0	V	
RF Input Power (P_{IN})	-	10	W	at RF1, RF2 and RFC
Storage Temperature	-65	+150	°C	

Table B.7 Operating Ranges:

Parameter	**Min**	**Max**	**Unit**	**Comments**
RF Frequency (f)	0.5	2.5	GHz	
Common Port Bias Voltage (V_S)	-	-	-	Applied at either VS1 port or VS2
Control Voltages (V_1,V_2)	0 +2.5	+0.2 +3.5	V	RF path OFF state RF path ON state
Ambient Temperature	-30	+85	°C	

B.3 TWP2233 Specifications:

The TWP2233 is a SPDT RF switch, which has a fast switching speed of 12ns. It can work within the frequency range from 5MHz to 2 GHz, and it is driven by TTL logic. The specifications for the chip are summarized in table B.8.

Table B.8 Summary of TWP2233 Specifications

Characteristic		Typical $T_a = 25°$	Min/Max $T_a = -55°$ to $+85°$	
Frequency		5-2000 MHz	5-2000	MHz
Insertion Loss (dB)		1.5	2.0	Max
Isolation		43	40	Min
VSWR		1.25:1	1.75:1	Max
Dc	Vdc	+5.0	+5.0	Max
Bias	mA	0.01	0.05	
Switching speed (nsec)		12	20	Max

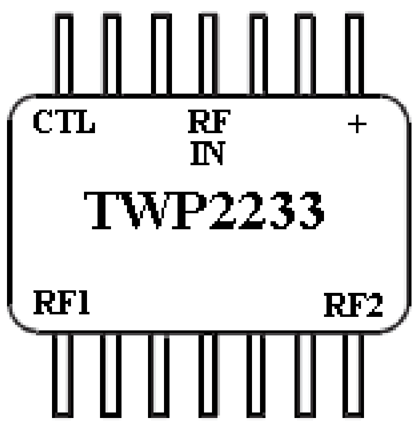

Figure B.3 TWP2233 Pin Layout

Table B.9 Truth Table for operation of TWP2233:

Control Input	Switch Condition	
TTL	RF Common to RF throw	
	RF1	RF2
0	ON	OFF
1	OFF	ON

B.4 TWH5017 Specifications:

The TWH5017 is a SP5T RF switch, which is reflective in the “OFF” state. It can work within the frequency range from 10MHz to 3 GHz, and it is driven by TTL logic. The specifications for the chip is summarized in table

Table B.10 Summary of TWH5017Specifications

Characteristic	**Typical** T_a **= 25°**	**Min/Max** T_a**= -55° to +85°**	
Frequency	10-3000 MHz	10-3000	MHz
Insertion Loss (dB)			
10-100 MHz	1.0	1.5	Max
100-1500 MHz	1.2	1.6	Max
1500-3000 MHz	1.4	2.4	Max
Isolation (dB)			
10-100 MHz	70	60	Min
100-1500 MHz	45	35	Min
1500-3000 MHz	35	30	Min
VSWR “ON”	1.3:1	1.6:1	Max
Switching speed (μsec)	2.0	3.0	Max

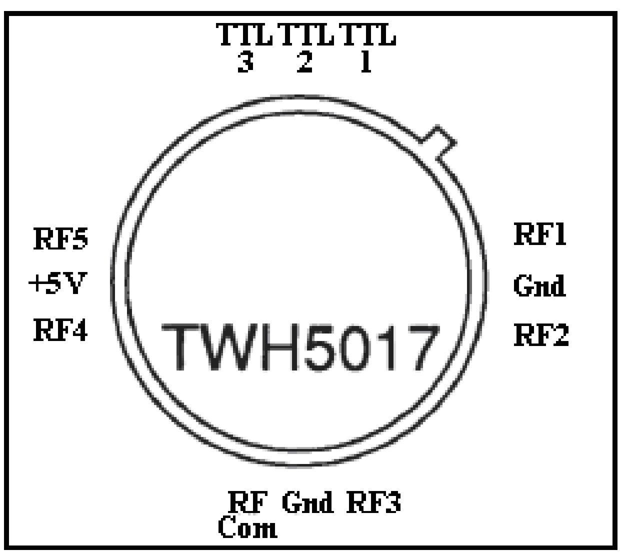

Figure B.4 TWH5017 Pin Layout

Table B.11Truth Table for operation of TWH5017:

TTL Control Inputs			**Switch Position**
TTL1	**TTL2**	**TTL3**	**RF Common Connected to**
0	0	0	RF1
1	0	0	RF2
0	1	0	RF3
1	1	0	RF4
0	0	1	RF5